Sphingosine-1-phosphate lyase is expressed by CD68+ cells on the parenchymal side of marginal reticular cells in human lymph nodes

ARTICLE *in* EUROPEAN JOURNAL OF IMMUNOLOGY · AUGUST 2014

Impact Factor: 4.03 · DOI: 10.1002/eji.201344158

European Journal of Immunology

Sphingosine-1-phosphate lyase is expressed by CD68$^+$ cells on the parenchymal side of marginal reticular cells in human lymph nodes

Saem Mul Park[*1,2], *Catherine E. Angel*[*1,2], *Julie D. McIntosh*[1,2], *Anna E. S. Brooks*[1,2], *Martin Middleditch*[1,2], *Chun-Jen J. Chen*[1,2], *Katya Ruggiero*[1], *Jonathan Cebon*[3] *and P. Rod Dunbar*[1,2]

[1] School of Biological Sciences, The University of Auckland, Auckland, New Zealand
[2] Maurice Wilkins Centre for Molecular Biodiscovery, The University of Auckland, Auckland, New Zealand
[3] Ludwig Institute for Cancer Research, Austin Health, Heidelberg, Melbourne, VIC, Australia

Lymph nodes (LNs) form the intersection between the vascular and lymphatic systems. Lymphocytes and antigen-presenting cells (APCs) traffic between these systems, but the barriers crossed during this trafficking in human LNs are poorly defined. We identified a population of cells in human LNs that lines the boundary between the parenchyma and lymphatic sinuses, consistent with descriptions of marginal reticular cells (MRCs) in murine LNs. Human MRCs are CD141^{high} podoplanin$^+$, CD90$^+$, ICAM1$^+$, and VCAM1$^+$ but lack endothelial and hematopoietic cell markers, or alpha-smooth muscle actin. We then examined expression of the enzyme sphingosine-1-phosphate (S1P) lyase (SGPL1) relative to the boundary defined by MRCs. SGPL1 expression was almost exclusively restricted to cells on the parenchymal side of MRCs, consistent with a role in maintaining the S1P gradient between the sinuses and the parenchyma. Surprisingly the cells expressing SGPL1 in the parenchyma were CD68$^+$ APCs. CD68$^+$ APCs generated from human monocytes were able to internalize and irreversibly degrade S1P, and this activity was inhibited by the S1P analogue FTY720. This work provides a map of the key structures at the boundary where human lymphocytes egress into sinuses, and identifies a novel potential mechanism for the activity of S1P analogues in humans.

Keywords: FTY720 · Lymph node · Lymphocyte egress · Marginal reticular cells · Sphingosine 1-phosphate

Additional supporting information may be found in the online version of this article at the publisher's web-site

Introduction

Lymph nodes (LNs) provide an interface between the blood and lymphatic systems, enabling presentation of antigen from the lymphatics to blood-derived lymphocytes. Understanding immune responses in human LNs requires better knowledge of the structural components and stromal cells with which immune cells interact. However, the cells and molecular pathways

Correspondence: Prof. P. Rod Dunbar
e-mail: r.dunbar@auckland.ac.nz

*These authors contributed equally to this work.

controlling lymphocyte migration within human LNs remain poorly characterized.

Data from rodent LNs suggest that the boundary between the cortex and the subcapsular sinus is lined by stromal cells dubbed marginal reticular cells (MRCs) [1]. During staining of human LNs for CD141 to identify CD141$^+$ CLEC9A$^+$ dendritic cells [2], we noted that CD141^{high} cells appeared in very similar locations to those reported for murine MRCs. In this work, we characterized these CD141^{high} cells by multicolor immunofluorescence microscopy, and confirmed by flow cytometry that a subpopulation of CD141$^+$ cells within human LNs bears the molecular hallmarks of MRCs.

Armed with the ability to identify MRCs, we were able to examine the boundaries where T-lymphocytes cross from parenchymal areas into lymphatic sinuses, and study some of the cells and molecules that control this egress. Trafficking into sinuses, which is crucial to the recirculation of lymphocytes, has been observed at both paracortical and medullary sites in rodent models [3–5]. In humans, lymphocyte egress into the sinuses is now a validated therapeutic target, with the advent into the clinic of the egress-blocking immunosuppressive drug FTY720 (Fingolimod).

Rodent models have demonstrated that sphingosine-1-phosphate (S1P) is involved in regulating lymphocyte egress into lymphatic sinuses [6–9]. S1P acts as a chemoattractant for lymphocytes expressing S1P receptors [6, 10]. In murine LNs, lymphatic endothelial cells (LECs) secrete S1P [11], and there is strong evidence that a gradient of S1P is generated across the boundary between the parenchyma and the sinuses, dependent on the function of S1P lyase (SGPL1) [10]. Inhibition, knock down, or knock out of SGPL1 results in elevated levels of S1P in the parenchyma and sequestering of lymphocytes in the LNs [10, 12–14]. However, the primary cell types that mediate S1P degradation by SGPL1 have not previously been identified in either rodent or human LNs [15].

FTY720, once phosphorylated in the body, is an S1P mimic and blocks lymphocyte egress either by down-regulating the responsiveness of lymphocytes to the S1P gradient or by interfering with the generation of the S1P gradient [3, 16]. Identifying the cells involved in modulating the S1P gradient across egress zones in human LNs might shed light on the mechanism of FTY720 action, and suggest new cellular and molecular targets for immunomodulatory drugs.

Here we identify a population of antigen presenting cells (APCs) that express SGPL1 in the T-lymphocyte-rich parenchyma of human LNs and then demonstrate that this type of human APC has the capacity to irreversibly degrade S1P.

Results

Identification and characterization of marginal reticular cells within human LNs

It has previously been reported that CD141/thrombomodulin marks a population of sinus endothelial cells and some perisinusal cells within human LNs [17]. Staining for CD141 revealed that a layer of CD141-bright cells lined a large proportion of the interface between the lymphatic sinuses, identified by nuclear staining for the LEC-specific homeobox transcription factor PROX1 [18], and the LN parenchyma (Fig. 1A–D). CD141^{high} cells lined the layers of PROX1$^+$ LECs forming the subcapsular and trabecular sinuses, but were not found on the sides of these sinuses occupied by fibrous tissue (Fig. 1A–C), indicating they were exclusively associated with the parenchymal cells. Given this specific location, particularly at the boundary between the subcapsular sinus and the outer parenchyma, these CD141^{high} cells fit the description of MRCs in murine LNs [1, 19]. Interestingly, although the MRC layer is exclusively found in the outer cortex underneath the subcapsular sinus in murine LNs, CD141^{high} cells also lined the trabecular, paracortical, and medullary sinuses in human LNs (Fig. 1A–D and Supporting Information Fig. 1). Subcapsular and trabecular sinuses could be distinguished not only by the presence of CD141^{high} cells and fibroblastic tissue on opposing edges of the sinuses, but also by the relative paucity of their lymphocyte content (Fig. 1E). Paracortical and medullary sinuses filled with APCs and T-lymphocytes were often completely encircled by CD141^{high} cells (Fig. 1F, Supporting Information Fig. 1), although gaps in the CD141^{high} partition were observed around some sinuses (Fig. 1F). The CD141^{high} partition around sinuses running through the paracortex (Fig. 1G) accounted for a small proportion of the total interface between T-lymphocyte-rich parenchyma and sinuses.

Simultaneous detection of CD141 with other cell specific markers clearly showed that CD141^{high} cells were distinct from CD3$^+$ T-lymphocytes or DCN46$^+$ APCs and LECs (Fig. 1E–I). The monoclonal antibody DCN46, although originally marketed as specific for CD209, has also been shown to detect LECs (by binding to L-SIGN [20]). This antibody was therefore used to identify both APCs and LECs in lymphatic sinuses in the paracortex and medulla. DCN46$^+$ cells were detected nestling among the CD141^{high} cells lining the trabecular sinus (Fig. 1E, right panels), and these had the morphology of APCs. Similarly, a few DCN46$^+$ cells were observed intercalated between the CD141^{high} cells surrounding the paracortical and medullary sinuses, whereas the majority was contained within the CD141^{high} barrier (Fig. 1F–I). A number of CD3$^+$ T-lymphocytes were also found traversing the CD141^{high} cell barrier surrounding these sinuses (Fig. 1F, H, and I), and many CD3$^+$ T-lymphocytes were observed among the DCN46$^+$ cells within the sinuses. Close inspection of the CD141^{high} cell layer suggested small portals or gates existed between the CD141^{high} cells (Fig. 1F, H, and I).

Costaining of CD141 with additional LEC markers [21] also confirmed that CD141^{high} cells represent a population distinct from PROX1$^+$, CD31$^+$, LYVE1$^+$, LECs (Fig. 1J and K, Supporting Information Fig. 1C). CD141^{high} cells were not detected in blood vessels (Fig. 1J, right panel), although occasionally small blood vessels did stain weakly for CD141 (Fig. 1K, right panels). In addition, a few lone CD141$^+$ cells were observed in the parenchyma and occasionally in the sinuses (data not shown); these lone CD141$^+$ are likely to represent the CD141$^+$CLEC9A$^+$

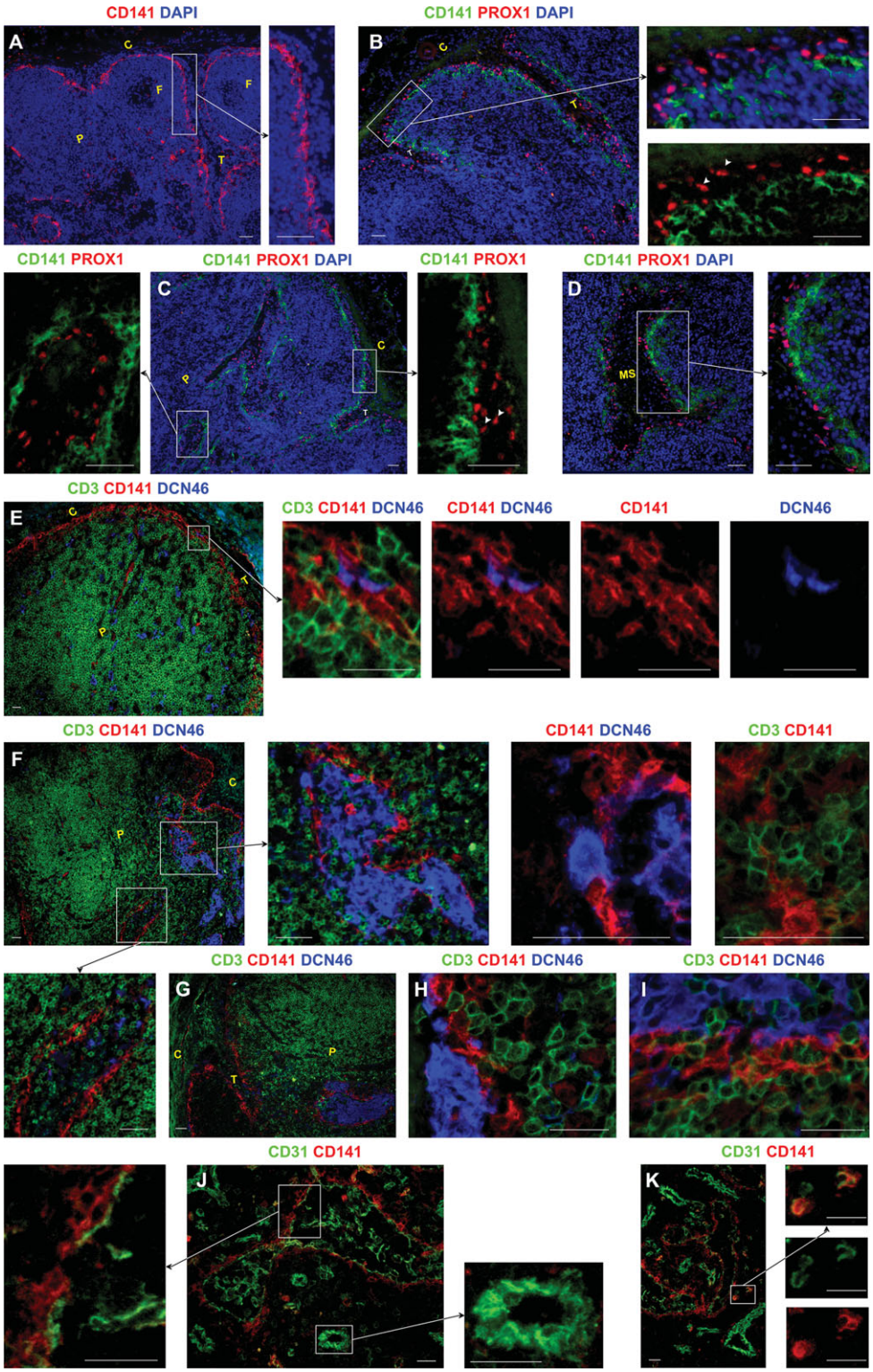

Figure 1. CD141^{high} cells line the parenchymal side of lymphatic sinuses in the human lymph node. Frozen human LN sections were examined by immunofluorescence microscopy for CD141 expression. (A) Images showing LN sections stained for CD141 (red) and DAPI (blue). (B–D) Representative images showing the distribution of CD141^{high} (green) cells relative to the PROX1^{+} (red) lymphatic sinuses in various locations. Arrowheads indicate the layers of PROX1^{+} cells in the subcapsular sinus. Blue represents DAPI staining of cell nuclei. (E–I) Images showing the localization of CD141^{high} cells (red), CD3^{+} T cells (green), and DCN46^{+} APCs and LECs (blue). (J–K) LN sections were costained for CD141 (red) and the pan-endothelial marker CD31 (green) to distinguish the MRCs from LECs and BECs (C, capsule; T, trabecula; F, follicle; P, paracortex; MS, medullary sinus). Scale bars represent 50 μm in (A–D) and (F and G) and 25 μm in (E) and (H–K). Data are representative of at least three independent experiments for each stain.

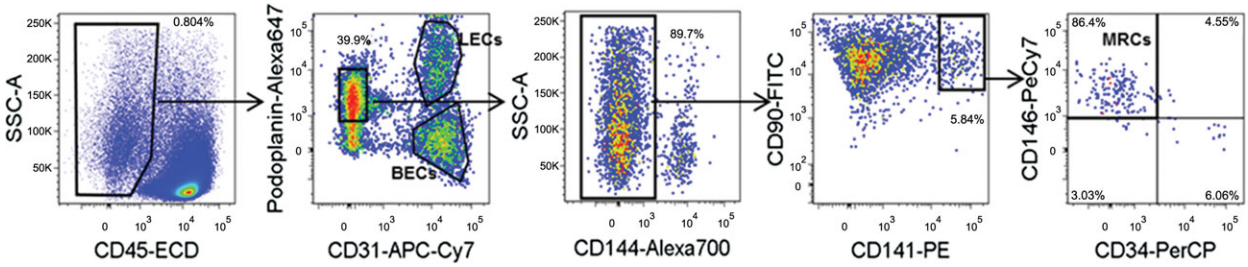

Figure 2. Identification of human MRCs by polychromatic flow cytometry. Human LN single-cell suspensions were analyzed by nine-color flow cytometry. CD141^{high} MRCs were identified after excluding hematopoietic and endothelial cells and gating on podoplanin$^+$ cells. Cell doublets were excluded by FCS-A/FSC-H and SSC-A/SSC-H, and dead cells were excluded by DAPI uptake (data not shown). Data shown are representative of three biological replicates.

APC population we previously identified in human LNs [2], as also characterized by others [22–24].

MRCs in rodents have a distinctive phenotype, expressing markers such as podoplanin, but lacking endothelial markers [1, 19]. To identify markers that definitively separate human MRCs from other stromal populations, we turned to nine-color flow cytometry of single-cell suspensions from human LNs (Fig. 2). A population of CD141^{high} cells that costained for the stromal markers CD90 and CD146 was revealed by excluding CD45$^+$, CD31$^+$, CD144$^+$, CD34$^+$ hematopoietic and endothelial cells, and then gating on podoplanin$^+$ cells (Fig. 2). Flow cytometry confirmed that MRCs are the brightest CD141$^+$ stromal population in single-cell suspensions from human LNs, are nonendothelial and nonhematopoietic, and coexpress CD90, podoplanin, and CD146.

MRCs in rodents also express adhesion molecules such as VCAM1/CD106, ICAM1/CD54, and MadCAM1 [1, 19]. Staining tissue sections for ICAM1 confirmed that CD141^{high} MRCs coexpressed ICAM1 (Fig. 3A), among a wide range of cells that stained for ICAM1 and VCAM1 (Fig. 3A and B). It was not possible to costain for CD141 and VCAM1 due to lack of suitable antibody isotypes; however, costaining for VCAM1 and ICAM1 showed that ICAM1$^+$ cells with the localization and morphology of MRCs were also VCAM1$^+$ (Fig. 3B). Staining for MadCAM1 by immunofluorescence microscopy was not technically robust and its expression by CD141^{high} MRCs was only occasionally observed (data not shown), although a previous study reported MadCAM1 expression by the VCAM1$^+$ cells located at the outer follicular region of human LNs [25]. CD141^{high} MRCs also colocalized with collagen and laminin (Fig. 3C and D), either due to expression of these proteins themselves or due to very close relationships to layers of extracellular matrix containing these components.

Costaining of tissue sections for podoplanin, CD141, and CD31 revealed that podoplanin expression by CD141^{high} MRCs was often weak compared with the other podoplanin$^+$ stromal populations (Fig. 3E and F). Antipodoplanin antibody brightly stained LECs and follicular dendritic cells (FDCs) (Fig. 3E and F), whereas CD141^{high} MRCs were stained weakly, consistent with our flow cytometry data (Fig. 2). MRCs could also be distinguished from stromal cells such as fibroblastic reticular cells (FRCs) by their lack of expression of α-smooth muscle actin (α-SMA) (Fig. 3G and H). α-SMA$^+$ FRCs were often intimately juxtaposed with MRCs (Fig. 3G, bottom panels). Finally, although RANKL has been reported as a marker for MRCs in mice [1], we were unable to detect RANKL expression in the CD141^{high} MRCs (data not shown).

Combining our immunofluorescence data with flow cytometry data, we conclude that MRCs in human LNs express CD141, CD90, ICAM1, VCAM1, and CD146, and can also express podoplanin to lower levels than LECs and FDCs, whereas they lack expression of CD45, CD34, CD31, CD144, and α-SMA; these markers are consistent with the molecular phenotype of rodent MRCs [19].

SGPL1 and the S1P transporter ABCC7 are expressed by CD68$^+$ APCs in the T lymphocyte-rich parenchyma

The ability to localize CD141^{high} MRCs and CD144$^+$ LECs [21, 26] allowed us to precisely define the boundary that separates the parenchyma from lymphatic sinuses. We thought S1P levels might be differentially regulated across this layer generating a gradient of S1P required for lymphocyte egress and therefore examined the two distinct regions demarcated by the MRC layer for expression of SGPL1, the enzyme irreversibly degrading S1P.

In all LNs studied, cells expressing high levels of SGPL1 were detected in the parenchyma (Fig. 4A–C), whereas such SGPL1$^+$ cells were mostly absent in the CD144$^+$ lymphatic sinuses. In one of the 12 LNs studied, rare SGPL1$^+$ cells were identified in the lymphatic sinuses, though these stained much less brightly than parenchymal SGPL1$^+$ cells (Fig. 4A). SGPL1 was not expressed by CD144$^+$ lymphatic or blood endothelial cells (Fig. 4A–C). All of the SGPL1^{high} cells in the parenchyma expressed CD68 (Fig. 4D and E), and the majority were DCN46$^+$ and/or CD169$^+$ (Fig. 4F and G). These SGPL1^{high} cells are therefore likely to represent the CD209^{low}CD68$^+$ and the CD209$^-$CD68$^+$ APCs we previously detected in the paracortex of human LNs [27].

In contrast, the majority of the CD68$^+$, DCN46$^+$, or CD169$^+$ cells in lymphatic sinuses expressed no detectable levels of SGPL1 (Fig. 4D–G). This stark contrast in SGPL1 expression is particularly clear in Figure 4E, where the CD68$^+$ APCs in the sinuses enclosed by the CD141^{high} MRC barrier lack SGPL1, while those outside the barrier in the parenchyma highly express SGPL1.

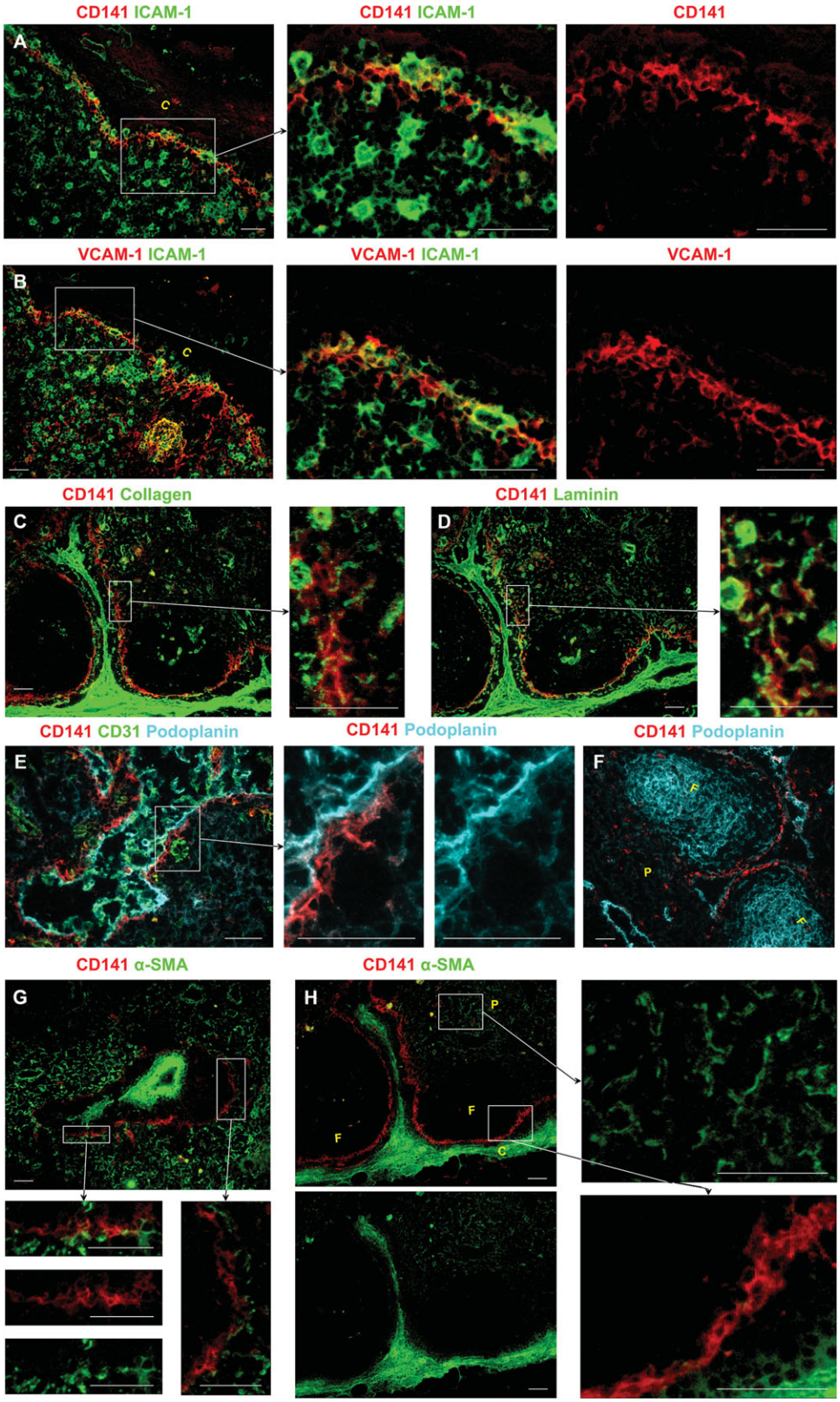

Figure 3. In situ phenotype of human MRCs. The molecular phenotype of CD141^{high} MRCs was examined by immunofluorescence microscopy. (A) Frozen LN tissues were stained for CD141 (red) and ICAM1 (green). (B) Representative images showing LN sections stained for VCAM1 (red) and ICAM1 (green). (C and D) LN sections were stained for CD141 (red), collagen, or laminin (green). (E and F) LN sections were costained for CD141 (red), CD31 (green), and podoplanin (cyan) to compare podoplanin expression by MRCs, LECs, and FDCs. (G and H) LN sections were stained for CD141 and the FRC marker α-SMA (C, capsule; F, follicle; P, paracortex). All scale bars represent 50 μm. Data are representative of at least three independent experiments for each stain.

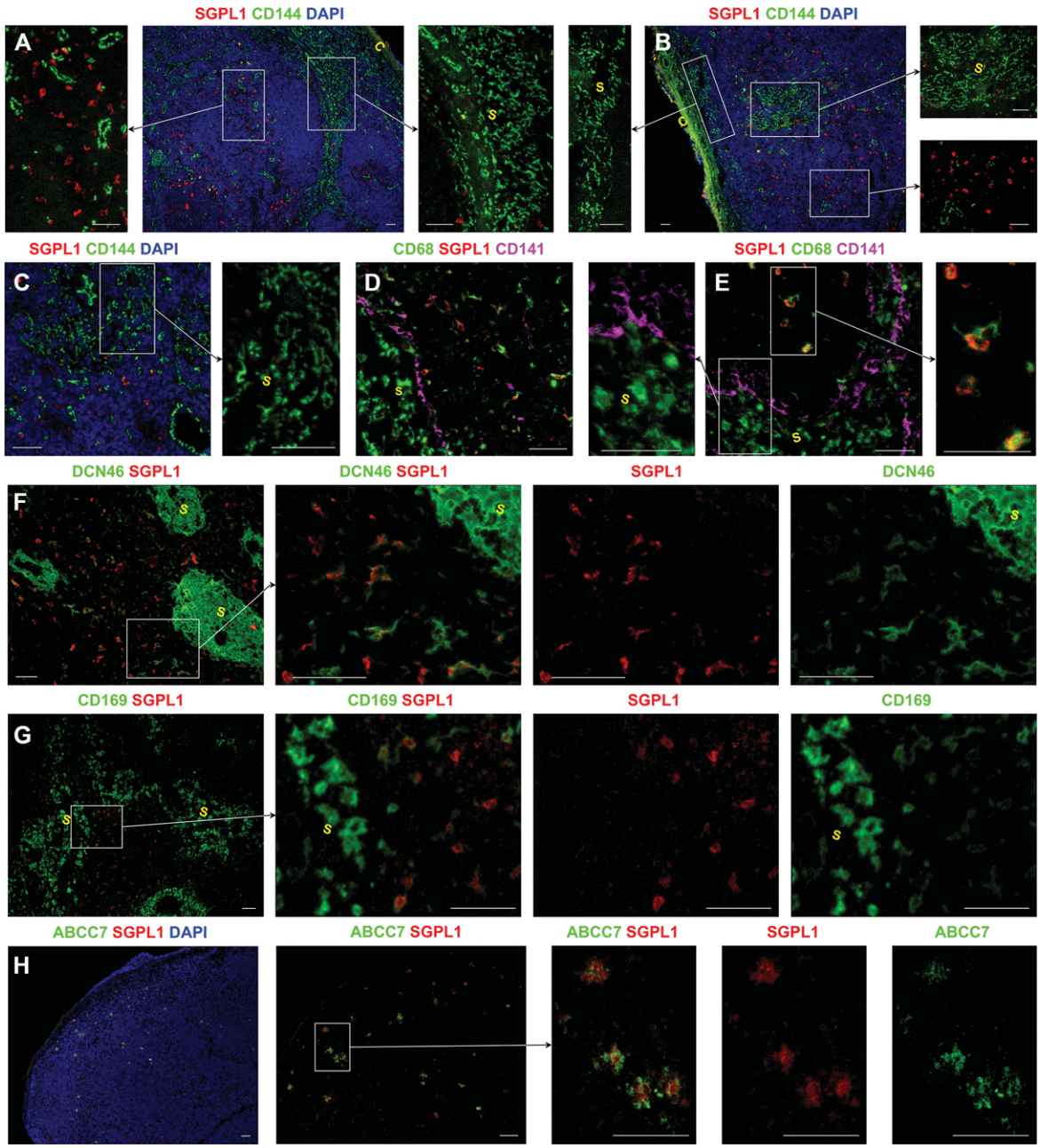

Figure 4. CD68$^+$ APCs in the parenchyma of the human lymph node express SGPL1 and the S1P transporter ABCC7. LN sections were examined by immunofluorescence microscopy for SGPL1 expression. (A–C) LN sections were stained for SGPL1 (red), CD144 (green), and DAPI (blue) to assess the distribution of SGPL1$^+$ cells relative to the CD144$^+$ lymphatic sinuses. (D and E) Images of LN sections costained for SGPL1 (red), CD68 (green), and the MRC marker CD141 (magenta). (F and G) Images showing costaining of SGPL1 (red) and the APC marker DCN46 or CD169 (green). (H) LN sections were stained for SGPL1 (red), DAPI (blue), and the S1P transporter ABCC7 (green; S, sinus). All scale bars represent 50 μm. Data are representative of three or more independent experiments.

In order for extracellular S1P to be irreversibly degraded by intracellular SGPL1, it must first be internalized. It has been reported that the ABC transporter ABCC7/CFTR can transport extracellular S1P inside the cell [28, 29]. We found the majority of SGPL1^{high} cells in the T lymphocyte-rich parenchyma also express ABCC7/CFTR (Fig. 4H). A summary of the phenotype of the SGPL1^{high} cells in the human LNs is shown in Supporting Information Table 1.

CD68$^+$SGPL1$^+$ APCs generated in vitro can internalize and irreversibly degrade extracellular S1P

We wanted to assess whether SGPL1^{high} APCs in the T lymphocyte-rich parenchyma could internalize and irreversibly degrade S1P. However, we could not identify any differences in the cell surface markers on CD68$^+$ APCs either side of the MRC barrier, and therefore could not use cell sorting to separate the SGPL1^{high}

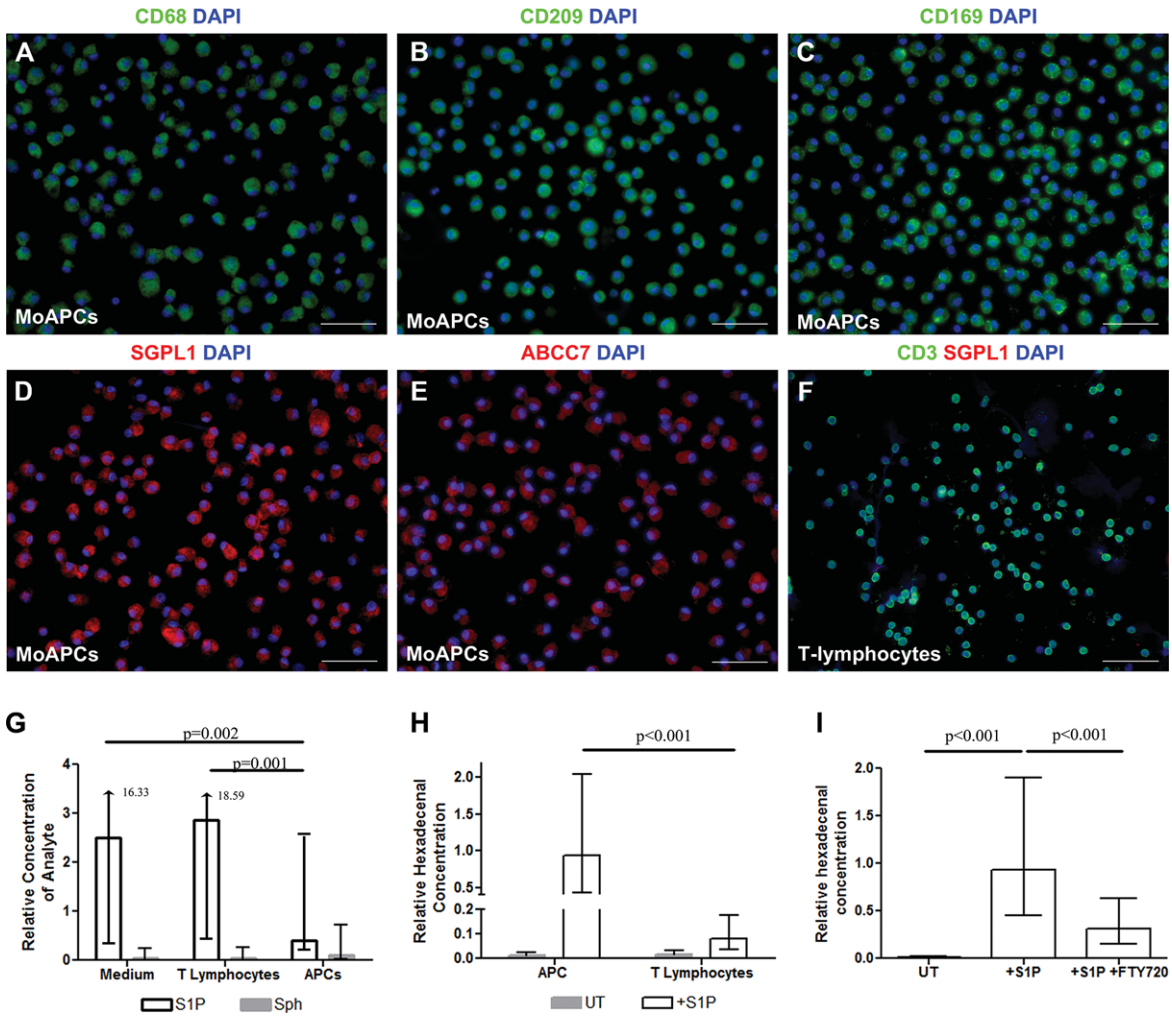

Figure 5. Human monocyte-derived CD68$^+$SGPL1$^+$ APCs can internalize S1P and degrade extracellular S1P. In vitro cultured MoAPCs were stained for (A) CD68, (B) CD209, (C) CD169, (D) SGPL1, (E) ABCC7, and DAPI. (F) T cells were costained for SGPL1, CD3, and DAPI. Data are representative of three independent experiments for each stain. Scale bars represent 50 μm. (G) The extracellular S1P (empty bars) and Sph (filled bars) concentration of MoAPCs and T lymphocytes was measured by mass spectrometry following incubation with extracellular C17 S1P. In (H), the hexadecenal concentration in the cell lysate of MoAPCs and T lymphocytes was measured following incubation with or without exogenously added S1P. Filled bars represent endogenous hexadecenal production; empty bars represent hexadecenal production following exogenous S1P addition. (I) Hexadecenal production of MoAPCs in the presence or absence of FTY720 was measured by mass spectrometry. In (G–I), the mean of three independent experiments, each with duplicate samples, is shown with 95% confidence intervals. The concentration of analyte was normalized to an internal standard and is shown as a relative concentration. Error bars correspond to 95% confidence intervals around the mean and end with an arrow, and the upper limit value (adjacent) for upper limits extending beyond the concentration range is shown on the graph. Statistical significance is indicated (t-test).

parenchymal APCs from the SGPL1$^{low/-}$ APCs in lymphatic sinuses. We therefore turned to a well characterized system for generating human APCs in vitro, and tested whether we could induce SGPL1^{high}ABCC7$^+$ APCs from monocytes. Using M-CSF, we generated APCs from human monocytes (MoAPCs) that expressed CD68, CD209, CD169, SGPL1, and ABCC7 (Fig. 5A–E), consistent with the SGPL1^{high} APCs in the T lymphocyte-rich parenchyma of human LNs. SGPL1 irreversibly degrades S1P into the long-chain aldehyde hexadecenal and ethanolamine-P [30]. The ability of MoAPCs to degrade S1P into hexadecenal was therefore examined, in comparison to T lymphocytes purified from blood that have no detectable expression of SGPL1 (Fig. 5F).

Since SGPL1 is located in the endoplasmic reticulum, degradation of extracellular S1P by this enzyme requires transport of the S1P into the cytoplasm. To determine whether MoAPCs were able to internalize S1P, the cells were incubated in the presence of S1P and the concentration of extracellular S1P was measured by mass spectrometry. To ensure that only exogenously added S1P was measured, C17-S1P was added to the cells rather than the endogenous C18-S1P. Following overnight culture with MoAPCs, the level of S1P remaining in the culture media was significantly reduced; in contrast, overnight culture with T lymphocytes induced no substantial change in S1P concentration (Fig. 5G). The decrease in extracellular S1P did not result in a concomitant increase in

sphingosine (Sph) in the medium, hence the decrease in S1P levels was not due to the activity of lipid phosphatases.

To determine whether the internalized S1P was degraded by SGPL1, the synthesis of hexadecenal in cellular lysates was measured as described previously [31]. Following incubation with S1P, low levels of hexadecenal were detected in T-lymphocyte lysate indicative of low levels of SGPL1 activity (Fig. 5H). By comparison, the level of hexadecenal in the MoAPC lysate was significantly elevated indicating a high rate of enzymatic activity in these cells (Fig. 5H). MoAPCs showed a greater than 50-fold increase in hexadecenal concentration relative to the untreated control (range 53–105%).

Finally FTY720, a known inhibitor of SGPL1 [31, 32], was shown to inhibit hexadecenal production in this system. Incubation of MoAPCs in the presence of S1P and FTY720 resulted in greater than 50% inhibition of SGPL1 activity (range 55–77%) (Fig. 5I).

Discussion

A better understanding of the structures controlling immune cell trafficking within human LNs is likely to lead to new insights into disease processes, and also improve the development of new immunomodulatory therapy. In this paper, we characterize the molecular phenotype and distribution of MRCs in human LNs. We then use this knowledge to study one of the key molecular systems controlling lymphocytes egress, and show that the S1P gradient from sinuses to parenchyma across the boundary constituted by MRCs is likely to be controlled by an unexpected cell type, $CD68^+$ APCs, within the parenchyma.

A barrier of cells expressing high levels of CD141 was detected at the interface between the lymphatic sinuses and neighboring parenchyma. A previous study observed CD141 expression on cells lining the sinus wall in human LNs, although this study concluded that these cells were LECs [17]. For the first time, we demonstrate that these $CD141^{high}$ cells represent a cell type distinct from $PROX1^+$ LECs, and that their phenotype is consistent with descriptions from murine studies of MRCs. It is interesting to note that $CD141^{high}$ MRCs in human LNs are found at the interface between the parenchyma and lymphatic sinuses in different locations (i.e., subcapsular, trabecular, paracortical and medullary sinuses), while the murine MRC layer is only found at the boundary between the outer cortex and the subcapsular sinus [1]. This may relate to the more complex structure of human LNs, including the presence of trabecular sinuses that are lacking in murine LNs.

Flow cytometry and/or immunohistochemistry revealed that $CD141^{high}$ MRCs express CD90, and adhesion molecules such as ICAM1, VCAM1, and MCAM/CD146. They can also express podoplanin, although they lack hematopoietic and endothelial markers, and α-SMA. Our data therefore cast human MRCs in a similar light to murine MRCs, as part of a related group of stromal cells including FRCs and FDCs that probably derive from lymphoid tissue organizer cells or their mesenchymal precursors [19]. Although CD141 is not exclusively expressed by human MRCs, the brightness of the CD141 signal allows it to be used as an MRC marker in multicolor immunofluorescence microscopy, due to the distinctive localization of MRCs at the boundaries between the parenchyma and the sinuses. Where the cortical parenchyma abuts the subcapsular or trabecular sinuses, $CD141^{high}$ MRCs surround the parenchyma on the side of the sinuses that does not contain fibrous tissue. Where fingers of medullary sinuses intercalate into the parenchyma, the $CD141^{high}$ MRCs appear to wrap these fingers of medullary sinuses. (In contrast, $CD141^+CLEC9A^+$ APCs appear as single discrete cells, mainly within the parenchyma, as we have published previously [2]). $CD141^{high}$ MRCs therefore form part of the barrier that lymphocytes must negotiate in order to exit the parenchyma into the sinuses. In high power images, T lymphocytes can be seen intercalating between MRCs, presumably moving from the parenchyma into the lymphatic sinuses to exit the LN [8]. The "portals" constituted by the gaps in the MRC barrier could be an important point of egress control, consistent with the stromal portals proposed by some authors in seeking to explain the mechanism of action of S1P and its analogues [7, 8, 33]. Interestingly $DCN46^+$ APCs were also often observed inside small portals in the $CD141^{high}$ MRC partition. Hence it is also conceivable that gaps between MRCs represent "gates" for APC migration from the sinuses into the lymphocyte-rich parenchyma.

The characterization of human MRCs now enables studies of their structure and function in normal human physiology and in disease, and it seems likely they will play a significant role in controlling trafficking of lymphocytes and perhaps APCs. In mice, MRCs are not only present in the LNs but also found at particular sites in various secondary lymphoid organs including the spleen, Peyer's patches, and nasal-associated lymphoid tissues [1]. It is currently unknown whether MRCs are also present in such organs in humans. Interestingly, a previous study reported CD141 staining on fibroblasts delineating the outer marginal zone in the human spleen [34]. Another fascinating question for future research is why MRCs should express such high levels of CD141, a cofactor for thrombin-mediated activation of protein C [35].

Having identified MRCs in relation to LECs, we were able to unequivocally determine sites of potential T-lymphocyte migration from the parenchyma into the sinuses. These sites are currently of major interest since trafficking of lymphocytes across these sites is now an accessible drug target, with the advent of the S1P analogue FTY720 into the clinic. S1P is believed to be involved in regulating the movement of T lymphocytes into the lymphatic sinuses and hence their subsequent egress from the LNs [6–9]. SGPL1 has a key role in generating a gradient of S1P from the sinuses to the parenchyma since inhibition of SGPL1 results in increased S1P levels in the LN parenchyma, and lymphocytes subsequently sequestrate in the LN causing lymphopenia [10, 12–14]. However, the primary cell types degrading S1P by SGPL1 in the parenchyma have not previously been identified.

Here for the first time we demonstrate that $CD68^+$ APCs in the T lymphocyte-rich parenchyma of the human LN express high levels of SGPL1. In contrast, lymphatic sinuses, where S1P is abundantly produced by LECs, lack $SGPL1^{high}$ APCs. Furthermore we

demonstrate that these CD68$^+$ APCs in the T lymphocyte-rich parenchyma express the ABC transporter ABCC7, which is capable of transporting extracellular S1P into the cell [28, 29], so it can be degraded by SGPL1 in the endoplasmic reticulum [36] and possibly the mitochondria [37]. Some of these CD68$^+$ APCs express CD169 and CD209, marking them as the parenchymal equivalents of sinus APCs [27]; crucially CD68$^+$ sinus APCs do not express detectable levels of either SGPL1 or ABCC7.

To establish whether these APCs are functionally capable of internalizing and degrading S1P, we generated CD68$^+$CD209$^+$ CD169$^+$SGPL1$^+$ABCC7$^+$ APCs from peripheral blood monocytes. Following culture with S1P, these MoAPCs substantially reduced the amount of S1P in the culture media; it is unclear yet whether the observed internalization of S1P is mediated by ABCC7 or by other S1P receptors expressed by MoAPCs [38, 39]. As earlier studies had proposed that extracellular S1P could be dephosphorylated by S1P phosphatase yielding sphingosine [40, 41], we also measured the sphingosine concentrations in the culture media. The sphingosine levels remained low indicating that S1P had not been dephosphorylated. We then demonstrated that S1P incubated in the presence of the MoAPCs was degraded into hexadecenal — a metabolic product specific to SGPL1 degradation of S1P. Finally, we demonstrated that FTY720 inhibited the SGPL1 activity in MoAPCs, supporting the hypothesis that SGPL1 inhibition by this drug may contribute to the lymphopenia it induces [32].

These findings place APCs at the centre of generating a crucial gradient for lymphocyte egress, and suggest that the flow of lymphocytes through the parenchyma into the sinuses may depend on both the numbers of these APCs present and their expression levels of SGPL1. Interestingly, it was recently shown in a murine system that CD8α^+ dendritic cells in the T-lymphocyte zone contribute to regulating oxysterol gradients required for activated B-lymphocyte trafficking by degrading oxysterol and thereby maintaining the T-lymphocyte zone as a low-oxysterol niche [42]. Future experiments, especially in the sophisticated mouse models available, will determine the interplay between APCs in the cortical parenchyma and T-lymphocyte egress, especially the factors capable of modulating SGPL1 expression by APCs.

Our data provide new markers and maps of the lymphatic sinuses and MRCs in human LNs that will enable new studies of human LNs in health and disease. As a first test of the utility of these markers, we have examined the expression of SGPL1 on either side of the boundary constituted by MRCs between the cortical parenchyma and the sinuses. These results point to CD68$^+$ APCs being an unexpected cell type likely to have a major effect on T-lymphocyte trafficking across this boundary, and a new cell type potentially targeted by the immunosuppressive drug FTY720.

Materials and methods

Human tissues

LNs were obtained from donors undergoing surgery and donors postmortem. The LNs assessed were from the axillary, inguinal, cervical, porta hepatis, parotid, and mesenteric node fields (Supporting Information Table 2). Patients or the next of kin gave written informed consent, under protocols approved by the Austin Health Human Research Ethics Committee, Heidelberg, Melbourne, and the Northern Regional Ethics Committee, New Zealand.

Multicolor immunofluorescence microscopy

LNs were embedded in TissueTek OCT compound (Sakura Finetek), snap frozen in liquid nitrogen and sectioned using a cryostat. Sections of length 5 μm were fixed with ice-cold acetone, blocked with 0.25% casein, and probed with the primary antibodies listed in Supporting Information Table 3. The monoclonal antibody DCN46 was used to identify lymphatic sinuses in the paracortex and medulla [43]; although this antibody is marketed as specific for CD209, it also stains L-SIGN [20], a molecule expressed by LECs in human LNs [44]. Primary antibodies were detected with the corresponding isotype specific goat antimouse, goat antirat, goat anti-FITC, or goat antirabbit secondary antibodies conjugated to a fluorophore (Alexa 350, 488, 555, or 647; Invitrogen). DAPI was included at 0.0005% w/v with secondary antibody. A different method was used when detecting ABCC7 expression; LNs were fixed with 4% PFA and treated with 0.1% Triton prior to antigen retrieval as previously described [45]. The slides were mounted using Prolong Gold (Invitrogen). Sections were visualized with a DMRE fluorescent microscope (Leica). Images were generated using Cytosketch (CytoCode).

Preparation of LN-cell suspensions

Mesenteric LNs were cut into small pieces and digested at 37°C for 20–60 min in RPMI 1640 (Gibco-BRL) containing Liberase DH (0.2 mg/mL; Roche) and DNaseI (100 units/mL; Sigma). The enzymes were replenished three times and the suspension was gently pipetted to facilitate tissue dissociation. The remaining tissue was then mechanically dissociated with a gentleMACS Dissociator (Miltenyi Biotec). To generate a single-cell suspension, the enzyme and mechanically generated preparations were combined, passed through a 75 μm nylon mesh and cryopreserved.

Flow cytometry

LN cell suspensions were thawed, washed, and incubated in RPMI 1640 containing 10% fetal bovine serum (Gibco-BRL) and 50 U/mL Benzonase Nuclease (Merck/Novagen) for 1 h. Cells were resuspended in PBS containing 1% human serum (BD Biosciences) and 1mM EDTA, and stained with the antibodies listed in Supporting Information Table 4 on ice for 30 min. DAPI (1:5000) was added prior to analysis. Samples were run on a Becton Dickinson FACS Aria II SORP, and data were analyzed using FlowJo V7.6.5.

Generation of human monocyte-derived APCs

Monocytes were isolated from PBMCs using the Monocyte Isolation Kit II (Miltenyi Biotec). MoAPCs were generated by culture in RPMI 1640 supplemented with 10% fetal bovine serum and 100 ng/mL M-CSF (Peprotech) for 6 days. MoAPCs were fixed with acetone at −20°C, blocked with 0.25% casein and stained with antibodies as described in the "*Multicolor Immunofluorescence Microscopy*" section.

Isolation of T lymphocytes from human blood

Peripheral blood T lymphocytes were isolated from PBMCs by the Pan T isolation Kit II (Miltenyi Biotec). T lymphocytes were rested in RPMI 1640 containing 5% human serum and 5 ng/mL IL-7 (Peprotech).

Measuring S1P internalization and metabolism by SGPL1$^+$ CD68$^+$ APCs

300–500 nM C17-S1P (Avanti Polar Lipids) was added to $\sim 3.5 \times 10^5$ MoAPCs or T lymphocytes in OpTmizer medium (Invitrogen) and cultured for 18 h. Supernatants were aspirated, and the lipid fraction was extracted. (2E)-hexadecenal was measured according to the method described previously [31] with slight modification. Cell lysates were incubated for 20 min with S1P ± FTY720 (Cayman Chemical) or left untreated. Following quenching of the reaction, the concentrations of the indicated analytes were determined by liquid chromatography–mass spectrometry (LC-MS) or liquid chromatography–tandem mass spectrometry (LC-MS/MS) on a QSTAR XL hybrid mass spectrometer (Applied Biosystems). Compound-specific fragment ion chromatograms were integrated for products of C18-S1P, C17-S1P, C18-Sphingosine, C17-Sphingosine, hexadecenal semicarbazide, and d5 hexadecenal semicarbazide using Analyst QS 2.0 (Applied Biosystems). Statistical analysis was performed using linear mixed models (LMMs) fitted to the natural log-transformed data. This approach takes account of the hierarchical structure of the physical material and variation they contribute to the observations, thereby enables the between subject variation to be eliminated prior to making comparisons being between cell types, analytes, and/or treatments. Log-transformation of the *d* was necessary in order for the data to meet the requisite underlying assumptions of LMMs. *t*-tests were carried out to assess the statistical significance of differences between pairs of means, and the resulting p-values were adjusted for multiple testing using Holm's method.

Acknowledgements: We gratefully acknowledge technical assistance from Dr Adrian Turner and Ms Judy Browning, and discussions regarding S1P metabolism with Dr Scott Graham. For donated clinical material we thank the staff and patients of the Austin Hospital (Melbourne) and Auckland City Hospital, especially Mr Adam Bartlett (New Zealand Liver Transplantation Unit). This work was supported by grants awarded to Professor P. Rod Dunbar from the Health Research Council of New Zealand (9141/3623553); the Maurice Wilkins Centre (9431/48512), and the University of Auckland (9450/71709).

Conflict of interest: The authors declare no conflict of interest.

References

1 **Katakai, T., Suto, H., Sugai, M., Gonda, H., Togawa, A., Suematsu, S., Ebisuno, Y. et al.**, Organizer-like reticular stromal cell layer common to adult secondary lymphoid organs. *J. Immunol.* 2008. **181:** 6189–6200.

2 **Jongbloed, S. L., Kassianos, A. J., McDonald, K. J., Clark, G. J., Ju, X., Angel, C. E., Chen, C. J. et al.**, Human CD141 +(BDCA-3)+ dendritic cells (DCs) represent a unique myeloid DC subset that cross-presents necrotic cell antigens. *J. Exp. Med.* 2010. **207:** 1247–1260.

3 **Mandala, S., Hajdu, R., Bergstrom, J., Quackenbush, E., Xie, J., Milligan, J., Thornton, R. et al.**, Alteration of lymphocyte trafficking by sphingosine-1-phosphate receptor agonists. *Science* 2002. **296:** 346–349.

4 **Takada, K. and Jameson, S. C.**, Naive T cell homeostasis: from awareness of space to a sense of place. *Nat. Rev. Immunol.* 2009. **9:** 823–832.

5 **Grigorova, I. L., Panteleev, M. and Cyster, J. G.**, Lymph node cortical sinus organization and relationship to lymphocyte egress dynamics and antigen exposure. *Proc. Natl. Acad. Sci. U S A* 2010. **107:** 20447–20452.

6 **Matloubian, M., Lo, C. G., Cinamon, G., Lesneski, M. J., Xu, Y., Brinkmann, V., Allende, M. L. et al.**, Lymphocyte egress from thymus and peripheral lymphoid organs is dependent on S1P receptor 1. *Nature* 2004. **427:** 355–360.

7 **Wei, S. H., Rosen, H., Matheu, M. P., Sanna, M. G., Wang, S.-K., Jo, E., Wong, C.-H. et al.**, Sphingosine 1-phosphate type 1 receptor agonism inhibits transendothelial migration of medullary T cells to lymphatic sinuses. *Nat. Immunol.* 2005. **6:** 1228–1235.

8 **Schwab, S. R. and Cyster, J. G.**, Finding a way out: lymphocyte egress from lymphoid organs. *Nat. Immunol.* 2007. **8:** 1295–1301.

9 **Rosen, H., Sanna, M. G., Cahalan, S. M. and Gonzalez-Cabrera, P. J.**, Tipping the gatekeeper: S1P regulation of endothelial barrier function. *Trends Immunol.* 2007. **28:** 102–107.

10 **Schwab, S. R., Pereira, J. P., Matloubian, M., Xu, Y., Huang, Y. and Cyster, J. G.**, Lymphocyte sequestration through S1P Lyase inhibition and disruption of S1P gradients. *Science* 2005. **309:** 1735–1739.

11 **Pham, T. H. M., Baluk, P., Xu, Y., Grigorova, I., Bankovich, A. J., Pappu, R., Coughlin, S. R. et al.**, Lymphatic endothelial cell sphingosine kinase activity is required for lymphocyte egress and lymphatic patterning. *J. Exp. Med.* 2010. **207:** 17–27.

12 **Bagdanoff, J. T., Donoviel, M. S., Nouraldeen, A., Tarver, J., Fu, Q., Carlsen, M., Jessop, T. C. et al.**, Inhibition of sphingosine-1-phosphate lyase for the treatment of autoimmune disorders. *J. Med. Chem.* 2009. **52:** 3941–3953.

13 **Vogel, P., Donoviel, M. S., Read, R., Hansen, G. M., Hazlewood, J., Anderson, S. J., Sun, W. et al.**, Incomplete inhibition of sphingosine 1-phosphate lyase modulates immune system function yet prevents early lethality and non-lymphoid lesions. *PLoS One* 2009. **4:** e4112.

14 **Spiegel, S. and Milstien, S.**, The outs and the ins of sphingosine-1-phosphate in immunity. *Nat. Rev. Immunol* 2011. **11:** 403–415.

15 **Cyster, J. G. and Schwab, S. R.**, Sphingosine-1-phosphate and lymphocyte egress from lymphoid organs. *Annu. Rev. Immunol.* 2012. **30:** 69–94.

16 **Brinkmann, V., Billich, A., Baumruker, T., Heining, P., Schmouder, R., Francis, G., Aradhye, S. et al.**, Fingolimod (FTY720): discovery and development of an oral drug to treat multiple sclerosis. *Nat. Rev. Drug Discov.* 2010. **9:** 883–897.

17 **Moll, R., Sievers, E., Hämmerling, B., Schmidt, A., Barth, M., Kuhn, C., Grund, C. et al.**, Endothelial and virgultar cell formations in the mammalian lymph node sinus: endothelial differentiation morphotypes characterized by a special kind of junction (complexus adhaerens). *Cell Tissue Res.* 2009. **335:** 109–141.

18 **Wilting, J., Papoutsi, M., Christ, B., Nicolaides, K. H., von Kaisenberg, C. S., Borges, J., Stark, G. B. et al.**, The transcription factor Prox1 is a marker for lymphatic endothelial cells in normal and diseased human tissues. *FASEB J.* 2002. **16:** 1271–1273.

19 **Katakai, T.**, Marginal reticular cells: a stromal subset directly descended from the lymphoid tissue organizer. *Front Immunol.* 2012. **3:** 200.

20 **Canard, B., Vachon, H., Fontaine, T., Pin, J.-J., Paul, S., Genin, C. and Mueller, C. G.**, Generation of anti-DC-SIGN monoclonal antibodies capable of blocking HIV-1 gp120 binding and reactive on formalin-fixed tissue. *Immunol. Lett.* 2011. **135:** 165–172.

21 **Park, S. M., Angel, C. E., McIntosh, J. D., Mansell, C. M., Chen, C. J., Cebon, J. and Dunbar, P. R.**, Mapping the distinctive populations of lymphatic endothelial cells in different zones of human lymph nodes. *PLoS One* 2014. **9:** e94781.

22 **Huysamen, C., Willment, J. A., Dennehy, K. M. and Brown, G. D.**, CLEC9A is a novel activation C-type lectin-like receptor expressed on BDCA3+ dendritic cells and a subset of monocytes. *J. Biol. Chem.* 2008. **283:** 16693–16701.

23 **Caminschi, I., Proietto, A. I., Ahmet, F., Kitsoulis, S., Shin Teh, J., Lo, J. C., Rizzitelli, A. et al.**, The dendritic cell subtype-restricted C-type lectin Clec9A is a target for vaccine enhancement. *Blood* 2008. **112:** 3264–3273.

24 **Poulin, L. F., Salio, M., Griessinger, E., Anjos-Afonso, F., Craciun, L., Chen, J. L., Keller, A. M. et al.**, Characterization of human DNGR-1+ BDCA3+ leukocytes as putative equivalents of mouse CD8alpha +dendritic cells. *J. Exp. Med.* 2010. **207:** 1261–1271.

25 **Onder, L., Narang, P., Scandella, E., Chai, Q., Iolyeva, M., Hoorweg, K., Halin, C. et al.**, IL-7-producing stromal cells are critical for lymph node remodeling. *Blood* 2012. **120:** 4675–4683.

26 **Baluk, P., Fuxe, J., Hashizume, H., Romano, T., Lashnits, E., Butz, S., Vestweber, D. et al.**, Functionally specialized junctions between endothelial cells of lymphatic vessels. *J. Exp. Med.* 2007. **204:** 2349–2362.

27 **Angel, C. E., Chen, C.-J. J., Horlacher, O. C., Winkler, S., John, T., Browning, J., MacGregor, D. et al.**, Distinctive localization of antigen-presenting cells in human lymph nodes. *Blood* 2009. **113:** 1257–1267.

28 **Boujaoude, L. C., Bradshaw-Wilder, C., Mao, C., Cohn, J., Ogretmen, B., Hannun, Y. A. and Obeid, L. M.**, Cystic fibrosis transmembrane regulator regulates uptake of sphingoid base phosphates and lysophosphatidic acid: modulation of cellular activity of sphingosine 1-phosphate. *J. Biol. Chem.* 2001. **276:** 35258–35264.

29 **Meissner, A., Yang, J., Kroetsch, J. T., Sauvé, M., Dax, H., Momen, A., Noyan-Ashraf, M. H. et al.**, Tumor necrosis factor-α–mediated downregulation of the cystic fibrosis transmembrane conductance regulator drives pathological sphingosine-1-phosphate signaling in a mouse model of heart failure. *Circulation* 2012. **125:** 2739–2750.

30 **Fyrst, H. and Saba, J. D.**, Sphingosine-1-phosphate lyase in development and disease: sphingolipid metabolism takes flight. *Biochim. Biophys. Acta.* 2008. **1781:** 448–458.

31 **Berdyshev, E. V., Goya, J., Gorshkova, I., Prestwich, G. D., Byun, H. S., Bittman, R. and Natarajan, V.**, Characterization of sphingosine-1-phosphate lyase activity by electrospray ionization-liquid chromatography/tandem mass spectrometry quantitation of (2E)-hexadecenal. *Anal. Biochem.* 2011. **408:** 12–18.

32 **Bandhuvula, P., Tam, Y. Y., Oskouian, B. and Saba, J. D.**, The immune modulator FTY720 inhibits sphingosine-1-phosphate lyase activity. *J. Biol. Chem.* 2005. **280:** 33697–33700.

33 **Sanna, M. G., Wang, S. K., Gonzalez-Cabrera, P. J., Don, A., Marsolais, D., Matheu, M. P., Wei, S. H. et al.**, Enhancement of capillary leakage and restoration of lymphocyte egress by a chiral S1P1 antagonist in vivo. *Nat. Chem. Biol.* 2006. **2:** 434–441.

34 **Steiniger, B., Stachniss, V., Schwarzbach, H. and Barth, P.**, Phenotypic differences between red pulp capillary and sinusoidal endothelia help localizing the open splenic circulation in humans. *Histochem. Cell Biol.* 2007. **128:** 391–398.

35 **Suzuki, K., Kusumoto, H., Deyashiki, Y., Nishioka, J., Maruyama, I., Zushi, M., Kawahara, S. et al.**, Structure and expression of human thrombomodulin, a thrombin receptor on endothelium acting as a cofactor for protein C activation. *EMBO. J.* 1987. **6:** 1891–1897.

36 **Ikeda, M., Kihara, A. and Igarashi, Y.**, Sphingosine-1-phosphate lyase SPL is an endoplasmic reticulum-resident, integral membrane protein with the pyridoxal 5'-phosphate binding domain exposed to the cytosol. *Biochem. Biophys. Res. Commun.* 2004. **325:** 338–343.

37 **Serra, M. and Saba, J. D.**, Sphingosine 1-phosphate lyase, a key regulator of sphingosine 1-phosphate signaling and function. *Adv. Enzyme. Regul.* 2010. **50:** 349–362.

38 **Weichand, B., Weis, N., Weigert, A., Grossmann, N., Levkau, B. and Brune, B.**, Apoptotic cells enhance sphingosine-1-phosphate receptor 1 dependent macrophage migration. *Eur. J. Immunol.* 2013. **43:** 3306–3313.

39 **Duong, C. Q., Bared, S. M., Abu-Khader, A., Buechler, C., Schmitz, A. and Schmitz, G.**, Expression of the lysophospholipid receptor family and investigation of lysophospholipid-mediated responses in human macrophages. *Biochim. Biophys. Acta.* 2004. **1682:** 112–119.

40 **Peest, U., Sensken, S. C., Andreani, P., Hanel, P., Van Veldhoven, P. P. and Graler, M. H.**, S1P-lyase independent clearance of extracellular sphingosine 1-phosphate after dephosphorylation and cellular uptake. *J. Cell Biochem.* 2008. **104:** 756–772.

41 **Johnson, K. R., Johnson, K. Y., Becker, K. P., Bielawski, J., Mao, C. and Obeid, L. M.**, Role of human sphingosine-1-phosphate phosphatase 1 in the regulation of intra- and extracellular sphingosine-1-phosphate levels and cell viability. *J. Biol. Chem.* 2003. **278:** 34541–34547.

42 **Yi, T., Wang, X., Kelly, Lisa M., An, J., Xu, Y., Sailer, Andreas W., Gustafsson, J. A. et al.**, Oxysterol gradient generation by lymphoid stromal cells guides activated B cell movement during humoral responses. *Immunity* 2012. **37:** 535–548.

43 **Engering, A., van Vliet, S. J., Hebeda, K., Jackson, D. G., Prevo, R., Singh, S. K., Geijtenbeek, T. B. H. et al.**, Dynamic populations of dendritic cell-specific ICAM-3 grabbing nonintegrin-positive immature dendritic cells and liver/lymph node-specific ICAM-3 grabbing nonintegrin-positive endothelial cells in the outer zones of the paracortex of human lymph nodes. *Am. J. Pathol.* 2004. **164:** 1587–1595.

44 **Pöhlmann, S., Soilleux, E. J., Baribaud, F., Leslie, G. J., Morris, L. S., Trowsdale, J., Lee, B. et al.**, DC-SIGNR, a DC-SIGN homologue expressed in endothelial cells, binds to human and simian immunodeficiency viruses and activates infection in trans. *Proc. Natl. Acad. Sci. USA* 2001. **98:** 2670–2675.

45 **Brown, D., Lydon, J., McLaughlin, M., Stuart-Tilley, A., Tyszkowski, R. and Alper, S.**, Antigen retrieval in cryostat tissue sections and cultured cells by treatment with sodium dodecyl sulfate (SDS). *Histochem. Cell Biol.* 1996. **105**: 261–267.

Abbreviations: **BEC**: blood endothelial cell · **FDC**: follicular dendritic cell · **FRCs**: fibroblastic reticular cell · **LEC**: lymphatic endothelial cell · **LN**: lymph node · **MoAPC**: monocyte-derived APC · **MRC**: marginal reticular cell · **S1P**: sphingosine-1-phosphate

Full correspondence: Prof. P. Rod Dunbar, School of Biological Sciences, Thomas Building, 3a Symonds Street, The University of Auckland, Auckland, New Zealand
Fax: +64-9-308-2317
e-mail: r.dunbar@auckland.ac.nz

Received: 10/10/2013
Revised: 31/3/2014
Accepted: 8/5/2014
Accepted article online: 13/5/2014

